

FED: Fast and Efficient Dataset Deduplication Framework with GPU Acceleration

Youngjun Son^{*†}

youngjun@aces.snu.ac.kr

Chaewon Kim^{*‡}

chaewon@aces.snu.ac.kr

Jaejin Lee^{†‡}

jaejin@snu.ac.kr

Abstract

Dataset deduplication plays a crucial role in enhancing data quality, ultimately improving the training performance and efficiency of large language models. A commonly used method for data deduplication is the MinHash LSH algorithm. Recently, NVIDIA introduced a GPU-based MinHash LSH deduplication method, but it remains suboptimal, leaving room for further improvement in processing efficiency. This paper proposes a GPU-accelerated deduplication framework, FED, that optimizes MinHash LSH for GPU clusters and leverages computationally efficient, partially reusable non-cryptographic hash functions. FED significantly outperforms the CPU-based deduplication tool in SlimPajama (using 64 logical CPU cores) by up to 107.2 times and the GPU-based tool in NVIDIA NeMo Curator by up to 6.3 times when processing 30 million documents on a node with four GPUs. Notably, our method dramatically accelerates the previously time-consuming MinHash signature generation phase, achieving speed-ups of up to 260 compared to the CPU baseline. Despite these gains in efficiency, FED maintains high deduplication quality, with the duplicate document sets reaching a Jaccard similarity of over 0.96 compared to those identified by the standard MinHash algorithm. In large-scale experiments, the deduplication of 1.2 trillion tokens is completed in just 6 hours in a four-node, 16-GPU environment. The related code is publicly available on GitHub (<https://github.com/mcrl/FED>).

1 Introduction

Pretrained language models (PLMs) (Vaswani et al., 2017; Raffel et al., 2020a; Brown et al., 2020a; Touvron et al., 2023a,b; Dubey et al., 2024) have

^{*}These authors contributed equally to this work

[†]Graduate school of Data Science, Seoul National University

[‡]Department of Computer Science, Seoul National University

demonstrated exceptional performance, enabling unprecedented various application advancements. It is well known that the larger the dataset, the better the PLM’s performance (Hoffmann et al., 2022; Rae et al., 2021a).

High-quality datasets are crucial for LLM training because they directly affect the language models’ performance, generalizability, and robustness (Gunasekar et al., 2023; Li et al., 2023). A critical aspect of ensuring data quality is the elimination of redundant data entries, a process known as *dataset deduplication*. Since datasets derived from internet dumps often contain many duplicate or near-duplicate documents (Elazar et al., 2024; Magnusson et al., 2023), it is important to consider that this redundancy in the training dataset can increase the time and resources required for LLM training (Sorscher et al., 2022). It may also introduce bias into the model’s learning process towards near-duplicates in the dataset (Lee et al., 2022).

Duplicate detection methods can be broadly categorized into two approaches: *exact matching*, which identifies cases where the text is completely identical or where the hash results of the text are the same, and *approximate matching*, which identifies documents with similar contents. Approximate matching is significantly more computationally expensive and time-consuming (Albalak et al., 2024). One commonly used approximate matching method is MinHash LSH (Indyk and Motwani, 1998), a simplified version of MinHash (Broder, 1997). However, widely adopted implementations of MinHash LSH are too slow to handle large-scale datasets effectively.

Recently, NVIDIA introduced NeMo-Curator (Jennings et al., 2024), a data processing tool with a GPU-accelerated deduplication tool. Although it is faster than traditional CPU-based implementations, tests in our hardware environment indicate that further enhancements are required for practical usability. In this context, we propose a

GPU-based deduplication framework called FED, which achieves fast processing without relying on high-end computational resources—thereby addressing the ever-growing scale of PLM datasets.

Our approach leverages a simple yet efficient hashing function and optimizes GPU kernel operations and communication. As a result, our framework can deduplicate a dataset of 1.2 trillion tokens in just 6 hours using 16 GPUs, each with 32GB of memory. The contributions of this paper are summarized as follows:

- **GPU-accelerated deduplication.** We present a new GPU-accelerated deduplication framework, called FED, optimized for computation and communication. Especially, it compares the document signatures in a matrix multiplication-like manner and exploits the existing GPU hardware units well. It also improves file I/O performance by exploiting parallelism to handle large-scale datasets.
- **Computationally efficient hash functions.** We introduce novel non-cryptographic hash functions that reduce computational cost by partially reusing the previous result during deduplication. As a result, FED can process the hash value generation part more than 260 times faster than the existing CPU baseline.
- **Stable deduplication quality.** By comparing the deduplication results of the widely used MinHash implementation with FED, we show that FED provides both speed and reliability in deduplication.
- **Publicly available code base.** We make the FED implementation publicly available. As LLMs continue to scale, FED will be instrumental in maintaining high data quality and enabling faster training cycles, ultimately advancing the field of NLP.

2 Background and Related Work

This section describes the background and related work to FED.

2.1 Effects of Data Deduplication

Data deduplication involves identifying and removing redundant data to ensure each instance is unique, enhancing a PLM’s learning efficiency and improving data quality. Figure 2 illustrates duplicate data within the RealNews (Zellers et al.,

2019) dataset. The sentence structures of the two documents are nearly identical, and such redundancy can hinder the effectiveness of learning for language models (LMs). Lee et al. (2022) suggests that dataset deduplication positively affects the validation perplexity of language models, and Allamanis (2019) presents that duplicated data in code datasets negatively affects LMs on code understanding tasks. Moreover, train-test leakage, where test data is inadvertently included in the training set, can significantly skew model evaluation metrics. For example, near-duplicates in both training and test datasets can lead to overestimating model performance. Thus, deduplication helps provide a more accurate assessment of model capabilities by eliminating these overlaps (Lee et al., 2022; Tirumala et al., 2023; Albalak et al., 2024).

Training on deduplicated datasets also reduces computational resource requirements, as the model processes unique information only once. This results in faster training times and lower costs (Sorscher et al., 2022). Deduplication also mitigates the risk of overfitting by preventing the model from memorizing repeated data entries, leading to better generalization of unseen data.

2.2 MinHash

MinHash (Broder, 1997) is a technique approximating the Jaccard similarity between two documents. Jaccard similarity (Jaccard, 1912), $J(A, B)$, is a metric to quantify the similarity of two finite sets, A and B :

$$J(A, B) = \frac{|A \cap B|}{|A \cup B|} \quad (1)$$

When used as a metric for finding document similarity, it is defined as the number of common words between the documents divided by the total number of words in them. While this is the most intuitive way to measure similarity, calculating the Jaccard similarity directly between documents in a large corpus is not feasible due to the computational cost. Thus, the MinHash algorithm (Broder, 1997), which approximates Jaccard similarity, is often used instead.

Identifying similar (duplicate) sets using MinHash can be broken down into four steps: MinHash generation, duplicate pair generation, constructing a union graph, and generating the final list of duplicates.

MinHash generation. Consider Figure 3. First, each document is broken down into smaller com-

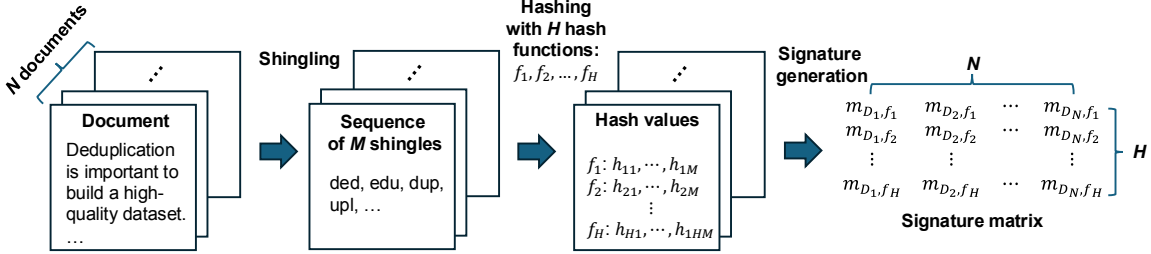


Figure 1: The process of MinHash generation.

RealNews Dataset	
index: 12347	text: Margins matter. The more Synovis Life Technologies (Nasdaq: SYNO) keeps of each buck it earns in revenue, the more money it has to invest in growth, fund new strategic plans, or (gasp!) distribute to shareholders. Healthy margins often separate pretenders from the best stocks in the market. That's why we check up on margins at least once a quarter in this series. ... (more)
index: 39083	text: Margins matter. The more Helen of Troy (Nasdaq: HELE) keeps of each buck it earns in revenue, the more money it has to invest in growth, fund new strategic plans, or (gasp!) distribute to shareholders. Healthy margins often separate pretenders from the best stocks in the market. That's why we check up on margins at least once a quarter in this series. ... (more)

Figure 2: Examples of duplicate documents.

ponents, known as *shingles* or *n-grams* and represented by the set of its shingles. Then, the shingles are mapped to zero or positive integers using H hash functions, f_1, f_2, \dots, f_H . As a result, we have H sequences of integers to represent a document. A MinHash signature for the document is a sequence of the minimum values obtained from each hash function, resulting in a sequence of length H . The Jaccard similarity between the two documents is then estimated by comparing their MinHash signatures. H different hash functions result in a $H \times N$ *signature matrix* for N documents. The choice of hash functions and the number of hash functions are critical hyperparameters in document deduplication based on MinHash.

For example, in Figure 1, the column 2 in the signature matrix is the signature of document D_2 . For D_2 , the minimum value of the hash values by the hash function f_1 is m_{D_2,f_1} , by f_2 is m_{D_2,f_2} , and so on. The MinHash signatures are much smaller than the original sets of shingles, allowing efficient computation of similarity between documents. The

choice of hash functions and the number of hash functions are critical hyperparameters in document deduplication based on MinHash.

Duplicate pair generation. MinHash compares every pair of document signatures to determine if the two documents are similar (duplicates). MinHash approximates two documents D_1 and D_2 's similarity $sim_{doc}(D_1, D_2)$ with their signatures S_1 and S_2 's similarity $sim_{sig}(S_1, S_2)$:

$$sim_{doc}(D_1, D_2) \approx sim_{sig}(S_1, S_2). \quad (2)$$

Specifically, MinHash approximates the Jaccard similarity of two documents by counting the same elements in their two signatures element-wise:

$$sim_{sig} = \frac{\text{The \# of the same elements}}{\text{The \# of elements in a signature}} \quad (3)$$

To classify a pair of documents as duplicates, MinHash uses a similarity threshold value θ . If $sim_{sig}(S_1, S_2) > \theta$, the documents D_1 and D_2 are considered duplicates (i.e., similar).

Constructing a union graph. After generating the list of duplicate pairs, we construct a union graph that clusters the duplicate pairs into groups. In the union graph, each document is a node, and an edge exists between two nodes if they form a duplicate pair. The resulting graph is an acyclic undirected graph where each connected component represents a group of near-duplicate documents.

Generating the final list of duplicates. Based on the connected components identified in the previous step, we select a representative document (e.g., the document with the lowest document index) for each connected component to build the deduplicated dataset.

2.3 MinHash LSH

Since MinHash computes the similarity for every pair of documents, it leads to a significant computational cost. To solve this problem, MinHash

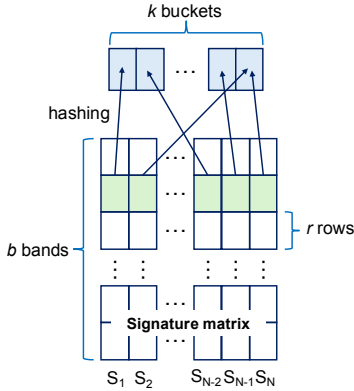


Figure 3: Hashing by MinHash LSH.

LSH combines MinHash with Locality-Sensitive Hashing (LSH) (Indyk and Motwani, 1998).

The critical difference between MinHash and MinHash LSH lies in the stage of generating duplicate pairs. In MinHash LSH, the signature column vector in the signature matrix of each document is divided into b bands, each of which has r integers. As shown in Figure 3, LSH hashes the bands in each document to k buckets. Let S_i be the signature vector of the document D_i . For a given signature vector S_1 and S_2 , when at least a pair of bands B_{S_1} from S_1 and B_{S_2} from S_2 hashed to the same bucket, we tag them as candidate pairs, potentially similar documents. For example, in Figure 3, D_2 and D_N are potentially similar documents because they have bands hashed to the same bucket. Then, LSH performs pairwise comparisons on each document's signature vectors of length $b \times r$ for the candidate pairs. If the similarity between the two vectors exceeds a predefined threshold, the two documents are considered a duplicate pair. Once the union graph is constructed for each band, the union graphs for all bands are merged to obtain the final union graph.

MinHash LSH is the most commonly used method for document deduplication (Albalak et al., 2024). Brown et al. (2020b) use MinHash LSH with ten hash functions to filter the training dataset for GPT-3. Rae et al. (2021b) use MinHash LSH with 13-grams and 450 hash functions for the gopher training dataset.

Despite MinHash LSH is an approximation of MinHash, it poses a significant computational and execution time burden. Surprisingly, previous studies have not seriously considered the time required for the deduplication process.

2.4 Existing MinHash LSH Implementations

The MinHash-LSH algorithm, implemented using the Python library *datasketch*, is widely used in many NLP studies. SlimPajama (Shen et al., 2023) employed CPU-based MinHash LSH using this library. We identified and fixed some bugs in their implementation, and hereafter, we will refer to this corrected version as the *CPU baseline* throughout the paper. The CPU baseline operates identically to the MinHash LSH process described in Section 2.3, with one key difference. The difference lies in how comparisons are performed between documents grouped into the same bucket. When a bucket contains B documents, comparisons are performed with a $O(B^2)$ time complexity. However, in the CPU baseline, comparisons are conducted between the first document's signature vector entering the bucket and those of subsequently arriving documents, resulting in $O(B)$.

Recently, NVIDIA introduced a framework called NeMo Curator (Jennings et al., 2024), which includes a GPU-accelerated MinHash LSH algorithm using cuDF (RAPIDS, 2024) and Dask libraries (Dask, 2024). We will refer to it as a *GPU baseline*. It is based on the approach used for Megatron-Turing NLG (Smith et al., 2022). Similar to the CPU baseline, it does not compare all pairs of documents within a bucket containing B documents. An anchor document for each bucket is selected, and the similarity between it and other documents in the bucket is computed. The GPU baseline is implemented using the Python GPU Data Frame library, cuDF, where document data is converted into a data frame format and processed with GPU-accelerated operations.

3 Design and Implementation of FED

We develop a deduplication framework, FED, optimized for GPU cluster environments where each node has multiple GPUs. It is capable of efficiently performing deduplication on massive datasets containing trillions of tokens. Considering scenarios where the size of the document set (e.g., trillions of tokens) exceeds the CPU and GPU memory capacity of the cluster, FED adopts a strategy to store intermediate results, such as the signature matrix and bucket IDs, on storage devices during the deduplication process. The overall process is illustrated in Figure 4.

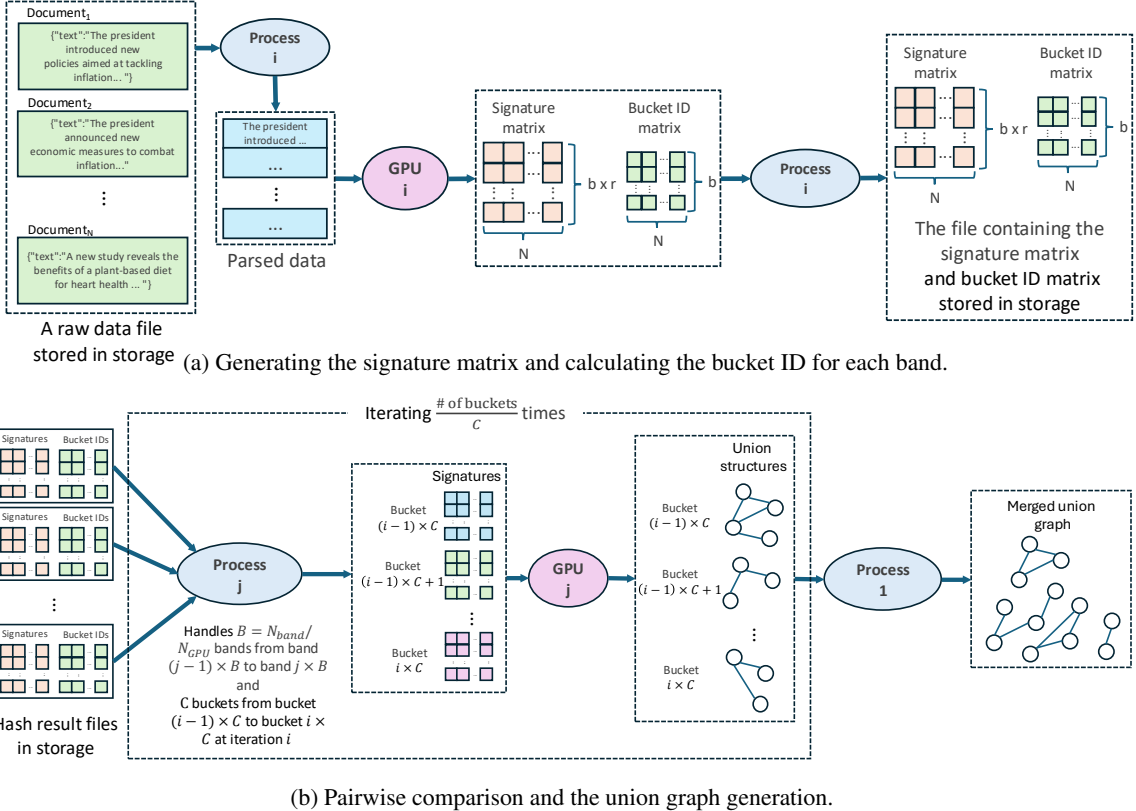


Figure 4: The overview of FED.

3.1 Overview of FED’s Minhash LSH

Assume that the raw dataset consists of multiple files and that they are stored in a suitable format, such as JSONL, as shown in Figure 4(a). Also, assume that each node in the cluster has N_{GPU} processes (each running in a CPU core) when N_{GPU} is the number of GPUs in each node. Each process reads and processes one file at a time. The file is loaded into the CPU’s main memory using two buffers according to a predefined format: one stores the text of all the documents in the file, and the other stores the document indices. These buffers are then transferred to the GPU. On the GPU, multiple CUDA (Luebke, 2008) threads generate the MinHash signature matrices for the documents in parallel and generate bucket ID for each band. The signature matrices and bucket ID matrices are transferred back to the CPU’s main memory and saved to a file. Consequently, each input file has a corresponding result file after hashing.

In MinHash LSH, documents sharing the same bucket ID are grouped together, and pairwise comparisons of their signature vectors are performed. As shown in Figure 4(b), process j scans all the hash result files and is in charge of $B = N_{band}/N_{GPU}$ bands from $(j-1) \times B$ to $j \times B$. For

each band, it extracts the document signatures with the same bucket ID and stores them in a separate buffer for the bucket ID. Due to the GPU memory limitation issues, each process handles C buckets at a time when scanning all the files and iterates until it covers all the buckets. The buffers are then transferred to the GPU for pairwise comparisons at each iteration. The similarity computation results are then transferred back to the CPU, where all the similar documents are connected to build the final union graph (by Process 1).

Unlike the CPU or GPU baseline implementation, which selects a representative document within a bucket containing B documents and performs comparisons in $O(B)$, FED compares all pairs of documents in the bucket in $O(B^2)$. Despite the increased number of comparisons, FED’s optimized GPU comparison kernel outperforms the existing methods. By performing more comparisons, we aim to reduce false negatives.

3.2 Hash Functions

MinHash LSH performs hashing twice. The first hashing involves calculating the MinHash values for each document to generate signature matrices. The second hashing assigns bucket IDs to the bands

of the signature vector of each document. The CPU and GPU baselines and FED differ in implementing these hashing steps.

Hashing in the CPU baseline The process of defining hash function h_i for MinHash generation in the CPU baseline is described as follows:

1. Set a large Mersenne prime $p = 2^{61} - 1$.
2. Generate two sequences of random numbers $\{a_i\}_{i=1}^H$ and $\{b_i\}_{i=1}^H$ such that $0 < a_i < p$ and $0 \leq b_i < p$.
3. $h_i = (a_i \times \text{SHA-1}(u) + b_i) \bmod p$,

where H is the number of different hash functions, and u refers to shingles composed of n -grams. CPU baseline uses a commonly used secure hash function SHA-1 (Eastlake 3rd and Jones, 2001), which is relatively slow when processing large data. LSH divides the signature vector of each document into b bands and hashes the values of each band into k buckets. In the CPU baseline, documents are mapped to the same bucket only if their signature vectors are identical in a particular band. As a result, the bucket size, k , tends to be very large in the CPU baseline.

Hashing in the GPU Baseline The primary focus of MinHash generation is preventing collisions rather than cryptographic security. However, the CPU baseline uses SHA-1 (Eastlake 3rd and Jones, 2001), which guarantees cryptographic security. The GPU baseline uses the non-cryptographic MurmurHash3 algorithm (Appleby, 2012) for MinHash generation. It produces a 32-bit or 128-bit hash value, enabling faster computation than SHA-1. In the LSH stage, the values of each band are mapped to buckets using the results of the MD5 hash function (Rivest, 1992), which generates a 128-bit fingerprint by encoding a string of any length.

Hashing in FED Unlike the CPU or GPU baseline, FED uses a computationally efficient and partially reusable non-cryptographic hash function for MinHash generation. Let $s = c_1 c_2 \dots c_k$ be a k -gram shingle that consists of characters and $f(s) = \sum_{i=1}^k c_i \cdot q^{i-1}$ such that q is a constant larger than the character alphabet size. Then FED's hash function $h(s)$ for MinHash generation is defined as follows:

$$h(s) = f(s) \bmod p \quad (4)$$

where p is a sufficiently large prime number. For example, we set $p = 4294967$ in our experiment. In this case, both p and q can be represented with 32-bit integers. Unlike SHA-1 and MurMurHash3 in the CPU and GPU baselines, the proposed hash function in Equation 4 allows reusing the hash value of the previous shingle. For example, let $t = c_2 \dots c_k c_{k+1}$ be the next k -shingle of a shingle $s = c_1 c_2 \dots c_k$. Then, $h(t)$ is computed as follows:

$$\begin{aligned} h(t) &= f(t) \bmod p \\ &= \left(\frac{f(s) - c_1}{q} + c_{k+1} q^{k-1} \right) \bmod p \end{aligned} \quad (5)$$

Instead of calculating $f(s)$ for each shingle, only a few operations – a single multiplication, two additions, and a single division – are necessary when computing the hash value of the next shingle with that of the current shingle. This significantly reduces the computational cost. Moreover, unlike SHA-1, FED's hash function is not constrained by the length of the string, making it more efficient for longer strings. We vary (p, q) pairs to generate multiple hash functions simultaneously, supporting parallel computation.

Number of Buckets in LSH For hashing to generate bucket IDs, FED sums the r values in each band and uses the remainder of the division by the pre-defined constant number of buckets, K . This effectively maps each band, which is defined in the space \mathbb{N}^r , into the space \mathbb{N}^K . As K increases, the process of scanning through files to group documents with the same key becomes more frequent. This process is proportional to K , resulting in $O(K)$. On the other hand, the number of documents with the same key is, on average, $O(\frac{N}{K})$ when N is the total number of documents. Since the comparison time is proportional to the square of the number of documents, the overall time complexity becomes $O\left(\left(\frac{N}{K}\right)^2 K\right) = O\left(\frac{N^2}{K}\right)$. Thus, the processing time can be approximated as $T(K) = aNK + \frac{bN^2}{K}$, where a and b are some constants. To minimize $T(K)$, we differentiate it with respect to K and set $\frac{dT(K)}{dK} = 0$, yielding $K^2 = \frac{bN^2}{aN}$. Solving for K , we find $K = \sqrt{\frac{b}{a}} N^{1/2}$. Thus, the optimal number of buckets can be expressed as $K = kN^{1/2}$, where $k = \sqrt{\frac{b}{a}}$ is a constant determined empirically. For example, we set k to 2 for 30B-token dataset. As the dataset size increases, it is recommended to use a larger k .

Suitability of FED’s Hash Functions In general, a good hash function for MinHash should have the following properties:

- **Determinacy:** The same input produces the same output.
- **Uniformity:** The hash function should distribute outputs uniformly across the range.
- **Collision resistance:** Two distinct inputs should unlikely produce the same hash value.

The proposed hash function satisfies these properties. Determinacy and uniformity are straightforward. Collision resistance is also met with a large value of p . When uniformity is satisfied, the probability of a collision approaches $\frac{1}{p}$, which is very small. In many contexts, hash functions are required to resist preimage attacks, making it computationally difficult to reverse-engineer the input from the hash value. However, it is not a concern in MinHash because the hash function is not used for security purposes.

3.3 GPU-based Pairwise Comparison

Given c documents in a bucket, each document has a signature vector S_i of the length equivalent to the number of hash functions used, where $i \in \{1, \dots, c\}$. For any pair (S_i, S_j) , we need to compute the following:

$$sim_{sig}(S_i, S_j) = \sum_k (S_{i,k} == S_{j,k}), \quad (6)$$

where $==$ is the equality operator.

Since typical GPU libraries do not support $sim_{sig}(S_i, S_j)$, we implement a custom GPU kernel. Replacing the equality operator ($==$) with the multiplication operator (\times) makes the operation matrix multiplication. Thus, the GPU kernel performs $sim_{sig}(S_i, S_j)$ in a matrix multiplication-like manner and runs much faster than the ordinary kernel that implements straightforwardly $sim_{sig}(S_i, S_j)$. The kernel exploits tiling and shared memory (Harris, 2012) to optimize memory access patterns and enhance parallel processing performance. When computing the Jaccard similarity for all c signature vectors in a pairwise manner, comparisons are performed only for pairs where $i < j$ to avoid redundant calculations. That is, instead of filling the entire $c \times c$ comparison result matrix, the computation is optimized to fill only the upper triangular matrix. Once the computation

is complete, the index information of document pairs exceeding the predefined similarity threshold is sent to the CPU.

3.4 Parallel File I/O Operations

To perform pairwise comparisons of document signatures, we need to gather all documents that belong to the same bucket. That is, we must search all the stored files to locate all documents that belong to a given bucket. As Section 3.1 mentions, each process reads the entire set of hash result files and then extracts the document signatures corresponding to the C bucket IDs, aggregating them into C separate buffers. That is, each process handles C bucket IDs concurrently, reducing the number of I/O operations. These buffers are then transferred to the GPU for pairwise comparisons. Each process iterates over buckets until all the buckets are handled. We choose C such that $(\frac{\text{Total size of files}}{K}) \times C \times N_{process}$ remains smaller than the available CPU memory, where $N_{process}$ is the number of processes at the CPU side in each node, and the total size of files is the sum of the sizes of all hash result files. K is the number of buckets, ensuring that the aggregated data for the C buckets fits within the system’s main memory. For example, when processing the RealNews dataset, we set $C = 4096$. The number of buckets processed per file I/O operation C is a tunable parameter. However, finding a suitable value that balances the CPU memory limits while sufficiently reducing the file I/O time is crucial.

Storing back hash results and bucket IDs Before the pairwise comparison step of signatures, we transfer the hash results and bucket IDs to the CPU as shown in Figure 4(a). If the CPU memory is insufficient, we store them in secondary storage, such as SSDs and HDDs, to address the issues in the target environment with a limited main memory space.

3.5 Other Optimizations

This section explains the optimization details when calculating signature matrices and generating duplicate pairs.

Initial Processing by the CPU The CPU processes handle different JSONL files in parallel. Each JSONL file is loaded into the CPU’s main memory using two buffers: one stores the text of all the documents in the file, and the other stores the document indices. After the buffers are filled

with a batch of files, the buffer is transferred to the corresponding GPU for shingling and MinHash generation. The size of the buffers depends on the capacity of the GPU memory.

Shingling and MinHash generation on the GPU

The GPU performs shingling and generates MinHash values for the documents contained in the buffer. Each JSONL file consists of multiple documents, and each Streaming Multiprocessor (SM) (Lindholm et al., 2008) within the GPU processes different documents independently. That is, a CUDA thread block processes a document, with each thread handling different MinHash functions.

Communication-computation overlapping

To maximize performance, we implement communication-computation overlapping techniques, such as double buffering (Cheng et al., 2014). When the GPU performs computation, a buffer containing a batch of files is simultaneously transferred to the GPU. Transferring data generated by the GPU back to the CPU is also overlapped with GPU computation.

Hash parameters for GPU compatibility The values for p and q described in Section 3.2 are carefully selected to address the limited support of the GPU’s 64-bit integer operations, ensuring that the result of the operation remains within the 32-bit integer range.

4 Experiment

This section compares FED against the existing CPU and GPU implementations of MinHash LSH.

4.1 Evaluation Environment

Target system configuration We use a 4-node GPU cluster with a storage node for our experiments. Each node is equipped with four NVIDIA Tesla V100 GPUs, with each GPU having 32GB of memory. Table 1 provides the detailed target system configuration.

Comparison baselines As mentioned in Section 2.4, the CPU baseline is the CPU-based MinHash LSH implementation found in SlimPajama (Shen et al., 2023). We identified and fixed some bugs in the implementation. The GPU baseline is the GPU-accelerated MinHash LSH implementation in NVIDIA NeMo Curator (Jennings et al., 2024).

For MinHash LSH, we use the default settings of the CPU baseline, 128 hash functions with $b = 16$

Table 1: System configuration of the 4-node GPU cluster

GPU node	
CPU	1 × AMD EPYC 7502 32-Core Processor
Memory	8 × 64GB DDR4 DIMM
GPU	4 × NVIDIA Tesla V100
OS	Ubuntu 20.04.6 (kernel 5.4.0-100)
Compiler	nvcc 12.4, GCC 9.4
GPU Driver	520.61.05
MPI Version	4.1
CUDA Version	12.4
Network Interface	InfiniBand (200Gb/s)
Storage node	
CPU	2 × AMD EPYC 7502 32-Core Processor
Memory	8 × 64GB DDR4 DIMM
RAID Configuration	RAID5, 7 × 3.7TB Sabrent Rocket 4.0 Plus NVMe SSDs, Max seq. read B/W per SSD: 7,000 MB/s, Max seq. write B/W per SSD: 5,800 MB/s, Max seq. read B/W of RAID5: 42,000MB/s, Max seq. write B/W of RAID5: 5,800 MB/s, Total capacity: 22.2TB
File System	ext4
Network Interface	InfiniBand (200Gb/s)

and $r = 8$. Following the approach by Lee et al. (Lee et al., 2022), we create shingles using five-grams and set the Jaccard similarity threshold to 0.8. The default settings of the CPU and GPU baselines are used for parameters other than the above-mentioned. As mentioned in Section 3.2, the number of buckets K is obtained based on the number of documents N , such that $K = 2N^{1/2}$.

Datasets used The datasets we used in our experiments are the RealNews dataset (Zellers et al., 2019) and C4 (Raffel et al., 2020b). The RealNews dataset is a large English corpus of news articles from Common Crawl, and C4 is a filtered version of Common Crawl. For C4, we sampled 100GB out of the total 700GB. We choose these datasets for two reasons. They are large-scale datasets containing over 30 million documents. We select a sufficiently large dataset to understand how long the traditional MinHash LSH method takes to process it and to see FED achieves how much acceleration. It is known from a previous study (Lee et al., 2022) that deduplication of the datasets we choose can improve the performance of language models.

Preprocessing the datasets Following SlimPajama (Shen et al., 2023), we preprocess the datasets before deduplication. We apply NFC normalization to remove non-Unicode characters, ensuring that a letter followed by a combining character becomes a single combined character. We also filter out documents with less than 200 characters.

Table 2: The deduplication time in seconds on a single node is compared across the CPU baseline, the GPU baseline, and FED. The CPU baseline uses 64 logical CPU cores. Both the GPU baseline and FED are evaluated using four GPUs in a single node.

Method	Dataset	Generation	Comparison	Union	Total	Speedup over CPU baseline	Speedup over GPU baseline
CPU baseline (SlimPajama (Shen et al., 2023))	RealNews (100 GB)	18,361.1	2,983.7	17.6	21,361.4	1.0	-
	Sampled C4 (100 GB)	22,748.4	3,878.8	33.1	26,660.3	1.0	-
GPU baseline (NVIDIA NeMo Curator (Jennings et al., 2024))	RealNews (100 GB)	361.5	864.4	30.5	1,256.4	17.0	1.0
	Sampled C4 (100 GB)	480.8	920.2	34.5	1,435.5	18.6	1.0
FED	RealNews (100 GB)	70.6	126.4	2.4	199.5	107.2	6.3
	Sampled C4 (100 GB)	91.7	243.9	2.6	338.2	78.8	4.2

4.2 Processing Speed

We measure three different types of execution time for deduplication speed comparison: signature generation and bucketing, signature comparison, and union. The signature generation and bucketing time involves computing the MinHash signature matrices and assigning bucket IDs for each band. The signature comparison time involves finding documents with the same bucket ID and calculating the Jaccard similarity between them. Finally, the union time involves constructing a union graph structure for all documents and ultimately identifying the documents to be removed.

We used the complete 100GB RealNews dataset and the sampled C4 dataset, which consists of 100GB randomly sampled from the full 750GB C4 dataset, for this experiment. The RealNews and sampled C4 datasets contain 32M and 50M documents, respectively. These datasets are constructed to be the same size, allowing us to evaluate how FED performs on datasets of equal size but with different characteristics. The deduplication experiment results for the full C4 dataset can be found in subsection 4.4.

When we measure the speed of the three deduplication methods, we flush page caches in the system to exclude their effect when performing file I/O. The CPU baseline processing time is measured using Python’s multiprocessing module across 64 logical CPU cores, while both the GPU baseline and FED are measured using four V100 GPUs in a single node. The results are summarized in Table 2. For deduplication on the RealNews dataset, FED is about 107.2 times faster than the CPU baseline and about 6.3 times faster than the GPU baseline. Notably, due to the introduction of reusable hash functions, the MinHash generation phase alone is roughly 260 times faster than the CPU baseline. Similarly, on the C4 dataset, FED achieves a speedup of 78.8 over the CPU baseline and about 4.2 over the GPU baseline.

For the comparison stage, FED is about 23.6

Table 3: Comparing the deduplication accuracy of the MinHash LSH-based approaches and the standard MinHash algorithm.

	0.1M documents		1M documents	
	Ratio	Jaccard	Ratio	Jaccard
Standard MinHash	7,317 / 0.1M	-	289,229 / 1M	-
CPU baseline	7,284 / 0.1M	0.995	288,683 / 1M	0.998
GPU baseline	7,144 / 0.1M	0.953	285,134 / 1M	0.976
FED	7,175 / 0.1M	0.956	283,248 / 1M	0.966

times faster than the CPU baseline and 6.8 times faster than the GPU baseline on RealNews. Similarly, on the C4 dataset, FED achieves a speedup of 15.9 over the CPU baseline and 3.8 over the GPU baseline. Moreover, as described in Section 3.1, FED performs more signature comparisons than others. While it is possible to reduce the number of comparisons by following the method used in the CPU or GPU baseline, the FED implementation prioritizes minimizing false negatives by performing more comparisons. The result indicates that the GPU kernel optimization for pairwise signature comparison described in Section 3.5 is very effective, and in turn performing more comparisons is feasible because of the optimized GPU kernels.

The processing speed of all methods is faster on the RealNews dataset than on the C4 dataset. It is attributed to the distinct characteristics of the two datasets. For both datasets, we use 100GB of data; however, RealNews consists of 32M documents with an average length of 3,335.17 characters (including spaces), whereas C4 consists of 50M documents with an average length of 2,191.15 characters (including spaces). Consequently, the higher number of documents in C4 increases the time taken for the generation and comparison phases.

4.3 Deduplication Accuracy

We verify if FED correctly identifies near-duplicate documents. Assuming that the result of MinHash, which performs pairwise comparisons on all document pairs, is the most accurate, we compare the indices of duplicated documents identified by the MinHash algorithm with those found by the CPU

and GPU baselines and FED.

We use a 0.1M and 1M dataset sampled from RealNews for this experiment because the original MinHash algorithm is time-consuming on large datasets. Our sampling is not entirely random to ensure many duplicated pairs even within the two smaller datasets. We first use MinHash LSH to identify similar groups, then select a proportion of each group to construct the subset.

In the deduplication process, duplicate pairs are identified and used to construct a union graph, from which groups of near-duplicate documents are formed. Each group consists of indices of similar (near-duplicate) documents. We define the set of all document indices with at least one near duplicate as *the set of all near duplicates*.

We evaluate the accuracy of the deduplication methods by measuring the Jaccard similarity between the set of all near duplicates obtained using the original and standard MinHash and that obtained using each method. A higher similarity indicates that the method identifies duplicate pairs more similarly to the standard MinHash.

Table 3 compares the deduplication accuracy of each method. The *Ratio* column represents the total number of documents that have near-duplicate pairs divided by the total number of documents. *Jaccard* column shows the Jaccard similarity between the sets of all near duplicates by the standard MinHash and each method. FED achieves a Jaccard similarity of 0.95 or higher to the standard MinHash result. A similarity score of 0.95 or higher means that the method has identified near-duplicate documents almost identically to the standard MinHash. In fact, on the 1M dataset, out of the 283,248 documents identified as having duplicate pairs by FED, 281,355 overlapped with those identified by MinHash. This indicates that FED not only achieves faster deduplication than other methods but also identifies near-duplicate documents similar to the standard MinHash.

4.4 Scalability

By varying the number of GPUs, the size of the dataset, and the number of hash functions used in MinHash generation, we evaluate the scalability of FED.

Number of GPUs. **Table 4** shows the results of measuring execution time when the number of GPUs is varying. Note that eight or more GPUs indicate a multi-node system configuration. We use

Table 4: Scalability with the number of GPUs (in seconds)

# of GPUs	1	2	4	8	16
Generation	92.9	81.3	70.6	53.6	46.9
Comparison	377.1	216.9	126.4	92.0	62.2
Union	1.5	2.0	2.4	2.4	2.6
Total Time	471.5	300.2	199.4	148.0	111.7

Table 5: Scalability with the dataset size (in seconds) using 16 GPUs

Dataset	Generation	Comparison	Union	Total
RealNews (30B tokens)	46.9	62.2	2.6	111.7
RedPajama-1T (1.2T tokens)	1436.4	20,275.4	35.4	21,747.2

Table 6: Scalability with the number of hash functions in FED on the 0.1M RealNews dataset

# of hash functions	# of bands	# of rows per band	Time (s)	Jaccard
128	16	8	2.3	0.956
256	16	16	2.3	0.924
512	32	16	3.7	0.943

the RealNews dataset, which has 32 million documents. Even with just a single GPU, the method is 45 times faster than the CPU baseline, and with 16 GPUs, the deduplication process completes in less than 2 minutes. This experiment demonstrates that our method works effectively in multi-node environments, and with more available node resources, even faster processing is possible.

Dataset size. We increase the dataset size to verify whether FED can process trillions of tokens at a practical processing speed. The results of deduplication using 16 GPUs on the RealNews and RedPajama-1T (Computer, 2023) datasets are shown in **Table 5**. It shows that FED can process trillions of tokens in just 6 hours. Since recent LLMs are typically trained with more than trillions of tokens, the results indicate that FED can be practically used to preprocess the training data for LLMs.

Number of hash functions. The number of hash functions used in the MinHash generation step is a key parameter that could impact the deduplication performance. For example, Rae et al. (2021b) use 450 hash functions. We vary the number of hash functions from 128 to 256 and 512, and **Table 6** shows the results. Despite changing the number of hash functions, FED maintained a Jaccard similarity of 0.92 or higher to the standard MinHash results, demonstrating that FED remains robust even with variations in the number of hash functions.

5 Conclusion

As the amount of data used for training LLMs continues to grow, the time required for data preprocessing has become increasingly significant. We present a framework called FED, which performs MinHash LSH-based deduplication efficiently on GPUs and uses novel hash functions. FED significantly outperforms the CPU-based deduplication tool (using 64 logical CPU cores) included in SlimPajama by up to 107.2 times and the GPU-based deduplication tool included in NVIDIA NeMo Curator by up to 6.3 times with a node of four GPUs when processing a dataset with 30 billion tokens. In a multi-node and multi-GPU environment, deduplication of 30 billion tokens by FED takes about 111.67 seconds and 1.2 trillion tokens about six hours. Similar documents identified by FED show a Jaccard similarity of 0.95 or higher with those found using the standard MinHash algorithm, indicating that FED achieves fast and accurate deduplication. Various experimental results highlight the practicality of FED for deduplication in large-scale datasets used for LLMs. We also make FED’s source code publicly available.

Acknowledgement

This work was supported in part by the National Research Foundation of Korea (NRF) grant (No. RS-2023-00222663, Center for Optimizing Hyper-scale AI Models and Platforms), by the BK21 Plus programs for Innovative Data Science Talent Education Program (Dept. of Data Science, SNU, No. 5199990914569) through NRF, by the Institute for Information and Communications Technology Promotion (IITP) grant (No. 2018-0-00581, CUDA Programming Environment for FPGA Clusters), all funded by the Ministry of Science and ICT (MSIT) of Korea. ICT at Seoul National University provided research facilities for this study.

References

Alon Albalak, Yanai Elazar, Sang Michael Xie, Shayne Longpre, Nathan Lambert, Xinyi Wang, Niklas Muennighoff, Bairu Hou, Liangming Pan, Haewon Jeong, et al. 2024. A survey on data selection for language models. *arXiv preprint arXiv:2402.16827*.

Miltiadis Allamanis. 2019. The adverse effects of code duplication in machine learning models of code. In *Proceedings of the 2019 ACM SIGPLAN International Symposium on New Ideas, New Paradigms, and Reflections on Programming and Software*, pages 143–153.

Austin Appleby. 2012. Murmurhash3, 2012. *URL: <https://github.com/aappleby/smhasher/blob/master/src/MurmurHash3.cpp>.*

Andrei Z Broder. 1997. On the resemblance and containment of documents. In *Proceedings. Compression and Complexity of SEQUENCES 1997 (Cat. No. 97TB100171)*, pages 21–29. IEEE.

Tom Brown, Benjamin Mann, Nick Ryder, Melanie Subbiah, Jared D Kaplan, Prafulla Dhariwal, Arvind Neelakantan, Pranav Shyam, Girish Sastry, Amanda Askell, et al. 2020a. Language models are few-shot learners. *Advances in neural information processing systems*, 33:1877–1901.

Tom Brown, Benjamin Mann, Nick Ryder, Melanie Subbiah, Jared D Kaplan, Prafulla Dhariwal, Arvind Neelakantan, Pranav Shyam, Girish Sastry, Amanda Askell, et al. 2020b. Language models are few-shot learners. *Advances in neural information processing systems*, 33:1877–1901.

John Cheng, Max Grossman, and Ty McKercher. 2014. *Professional CUDA c programming*. John Wiley & Sons.

Together Computer. 2023. [Redpajama: an open dataset for training large language models](#).

Dask. 2024. [Dask: a python library for parallel and distributed computing](#).

Abhimanyu Dubey, Abhinav Jauhri, Abhinav Pandey, Abhishek Kadian, Ahmad Al-Dahle, Aiesha Letman, Akhil Mathur, Alan Schelten, Amy Yang, Angela Fan, et al. 2024. The llama 3 herd of models. *arXiv preprint arXiv:2407.21783*.

D. Eastlake 3rd and P. Jones. 2001. [US Secure Hash Algorithm 1 \(SHA1\)](#). RFC 3174 (Informational). Updated by RFC 4634.

Yanai Elazar, Akshita Bhagia, Ian Magnusson, Abhilasha Ravichander, Dustin Schwenk, Alane Suhr, Pete Walsh, Dirk Groeneveld, Luca Soldaini, Sameer Singh, Hanna Hajishirzi, Noah A. Smith, and Jesse Dodge. 2024. [What’s in my big data? Preprint](#), arXiv:2310.20707.

Suriya Gunasekar, Yi Zhang, Jyoti Aneja, Caio César Teodoro Mendes, Allie Del Giorno, Sivakanth Gopi, Mojan Javaheripan, Piero Kauffmann, Gustavo de Rosa, Olli Saarikivi, et al. 2023. Textbooks are all you need. *arXiv preprint arXiv:2306.11644*.

Mark Harris. 2012. Using shared memory in cuda c/c++. <https://developer.nvidia.com/blog/using-shared-memory-cuda-cc/>. Accessed: 2024-12-15.

Jordan Hoffmann, Sebastian Borgeaud, Arthur Mensch, Elena Buchatskaya, Trevor Cai, Eliza Rutherford, Diego de Las Casas, Lisa Anne Hendricks, Johannes Welbl, Aidan Clark, et al. 2022. Training compute-optimal large language models. *arXiv preprint arXiv:2203.15556*.

Piotr Indyk and Rajeev Motwani. 1998. Approximate nearest neighbors: towards removing the curse of dimensionality. In *Proceedings of the thirtieth annual ACM symposium on Theory of computing*, pages 604–613.

Paul Jaccard. 1912. The distribution of the flora in the alpine zone. 1. *New phytologist*, 11(2):37–50.

Joseph Jennings, Mostafa Patwary, Sandeep Subramanian, Shrimai Prabhumoye, Ayush Dattagupta, Vibhu Jawa, Jiwei Liu, Ryan Wolf, Sarah Yurick, and Varun Singh. 2024. **NeMo-Curator: a toolkit for data curation.**

Katherine Lee, Daphne Ippolito, Andrew Nystrom, Chiyuan Zhang, Douglas Eck, Chris Callison-Burch, and Nicholas Carlini. 2022. **Deduplicating training data makes language models better.** In *Proceedings of the 60th Annual Meeting of the Association for Computational Linguistics (Volume 1: Long Papers)*, pages 8424–8445, Dublin, Ireland. Association for Computational Linguistics.

Yuanzhi Li, Sébastien Bubeck, Ronen Eldan, Allie Del Giorno, Suriya Gunasekar, and Yin Tat Lee. 2023. Textbooks are all you need ii: phi-1.5 technical report. *arXiv preprint arXiv:2309.05463*.

Erik Lindholm, John Nickolls, Stuart Oberman, and John Montrym. 2008. Nvidia tesla: A unified graphics and computing architecture. *IEEE micro*, 28(2):39–55.

David Luebke. 2008. Cuda: Scalable parallel programming for high-performance scientific computing. In *2008 5th IEEE international symposium on biomedical imaging: from nano to macro*, pages 836–838. IEEE.

Ian Magnusson, Akshita Bhagia, Valentin Hofmann, Luca Soldaini, Ananya Harsh Jha, Oyvind Tafjord, Dustin Schwenk, Evan Pete Walsh, Yanai Elazar, Kyle Lo, et al. 2023. Paloma: A benchmark for evaluating language model fit. *arXiv preprint arXiv:2312.10523*.

Jack W Rae, Sebastian Borgeaud, Trevor Cai, Katie Millican, Jordan Hoffmann, Francis Song, John Aslanides, Sarah Henderson, Roman Ring, Susan-nah Young, et al. 2021a. Scaling language models: Methods, analysis & insights from training gopher. *arXiv preprint arXiv:2112.11446*.

Jack W Rae, Sebastian Borgeaud, Trevor Cai, Katie Millican, Jordan Hoffmann, Francis Song, John Aslanides, Sarah Henderson, Roman Ring, Susan-nah Young, et al. 2021b. Scaling language models: Methods, analysis & insights from training gopher. *arXiv preprint arXiv:2112.11446*.

Colin Raffel, Noam Shazeer, Adam Roberts, Katherine Lee, Sharan Narang, Michael Matena, Yanqi Zhou, Wei Li, and Peter J Liu. 2020a. Exploring the limits of transfer learning with a unified text-to-text transformer. *Journal of machine learning research*, 21(140):1–67.

Colin Raffel, Noam Shazeer, Adam Roberts, Katherine Lee, Sharan Narang, Michael Matena, Yanqi Zhou, Wei Li, Peter J Liu, et al. 2020b. **Exploring the limits of transfer learning with a unified text-to-text transformer.** *J. Mach. Learn. Res.*, 21(140):1–67.

RAPIDS. 2024. **cudf - gpu dataframes**.

Ronald Rivest. 1992. Rfc1321: The md5 message-digest algorithm.

Zhiqiang Shen, Tianhua Tao, Liqun Ma, Willie Neiswanger, Joel Hestness, Natalia Vassilieva, Daria Soboleva, and Eric Xing. 2023. Slimpajama-dc: Understanding data combinations for llm training. *arXiv preprint arXiv:2309.10818*.

Shaden Smith, Mostafa Patwary, Brandon Norick, Patrick LeGresley, Samyam Rajbhandari, Jared Casper, Zhun Liu, Shrimai Prabhumoye, George Zerveas, Vijay Korthikanti, et al. 2022. Using deep-speed and megatron to train megatron-turing nlg 530b, a large-scale generative language model. *arXiv preprint arXiv:2201.11990*.

Ben Sorscher, Robert Geirhos, Shashank Shekhar, Surya Ganguli, and Ari Morcos. 2022. Beyond neural scaling laws: beating power law scaling via data pruning. *Advances in Neural Information Processing Systems*, 35:19523–19536.

Kushal Tirumala, Daniel Simig, Armen Aghajanyan, and Ari Morcos. 2023. D4: Improving llm pretraining via document de-duplication and diversification. *Advances in Neural Information Processing Systems*, 36:53983–53995.

Hugo Touvron, Thibaut Lavril, Gautier Izacard, Xavier Martinet, Marie-Anne Lachaux, Timothée Lacroix, Baptiste Rozière, Naman Goyal, Eric Hambro, Faisal Azhar, Aurelien Rodriguez, Armand Joulin, Edouard Grave, and Guillaume Lample. 2023a. **Llama: Open and efficient foundation language models.** *Preprint*, arXiv:2302.13971.

Hugo Touvron, Louis Martin, Kevin Stone, Peter Albert, Amjad Almahairi, Yasmine Babaei, Nikolay Bashlykov, Soumya Batra, Prajwal Bhargava, Shruti Bhosale, et al. 2023b. Llama 2: Open foundation and fine-tuned chat models. *arXiv preprint arXiv:2307.09288*.

Ashish Vaswani, Noam Shazeer, Niki Parmar, Jakob Uszkoreit, Llion Jones, Aidan N Gomez, Łukasz Kaiser, and Illia Polosukhin. 2017. [Attention is all](#)

[you need](#). *Advances in neural information processing systems*, 30.

Rowan Zellers, Ari Holtzman, Hannah Rashkin, Yonatan Bisk, Ali Farhadi, Franziska Roesner, and Yejin Choi. 2019. Defending against neural fake news. *Advances in neural information processing systems*, 32.